

Article

Mechanical Properties of Cement Mortars Reinforced with Polypropylene Fibers Subjected to High Temperatures and Different Cooling Regimes

Yorly Alvarez, María Isabel Prieto *  and Alfonso Cobo 

Tecnología de la Edificación, Universidad Politécnica de Madrid, 28040 Madrid, Spain;
y.alvarez@alumnos.upm.es (Y.A.); alfonso.cobo@upm.es (A.C.)

* Correspondence: mariaisabel.prieto@upm.es

Abstract: This study experimentally investigated the mechanical properties of cement mortars that were reinforced with polypropylene (PP) fibers after being exposed to high temperatures and cooled under different regimes. PP fibers were added in amounts of 2, 3 and 4 kg/m³, the residual strengths of the mortars exposed to various temperatures up to 500 °C and cooled under different regimes were determined. It was found that the addition of PP fiber at the level of 2 kg/m³ improves the residual flexural and compressive strengths up to 300 °C. The residual flexural strength was approximately 75%, which is 15% higher than that observed in the simple mortar, and the same happens with the residual compressive strength which was approximately 85%, which is 17% higher than that observed in the simple mortar, regardless of the types of cooling used on the specimens. It was determined by means of a statistical analysis that there are no significant differences in the mechanical properties of the mortar according to the cooling regimes used, after having been exposed to high temperatures. The correlation of the residual flexural and compressive strengths was achieved with a coefficient of determination, $R^2 = 0.82$, and the relationships between the variables were considered acceptable regardless of the types of cooling used.

Keywords: mortar; cement; fiber; polypropylene; temperature



Citation: Alvarez, Y.; Prieto, M.I.; Cobo, A. Mechanical Properties of Cement Mortars Reinforced with Polypropylene Fibers Subjected to High Temperatures and Different Cooling Regimes. *Buildings* **2023**, *13*, 1445. <https://doi.org/10.3390/buildings13061445>

Academic Editor: Binsheng (Ben) Zhang

Received: 8 May 2023

Revised: 27 May 2023

Accepted: 28 May 2023

Published: 1 June 2023



Copyright: © 2023 by the authors. Licensee MDPI, Basel, Switzerland. This article is an open access article distributed under the terms and conditions of the Creative Commons Attribution (CC BY) license (<https://creativecommons.org/licenses/by/4.0/>).

1. Introduction

Mortars are the result of a mixture of cement, water, aggregates and in some cases additives according to their dosages and utilities, which obtain the characteristics of high resistance and durability [1].

In recent years, research has been carried out to develop new materials or systems that can withstand the high temperatures that develop during a fire in a building [2–6]. The high temperatures produced during a fire is one of the most severe environmental loads experienced and is a challenge for the integrity and safety of structures [7]. Concrete is not combustible, making it more suitable for the protection of steel bars found in reinforced concrete structures, besides being one of the most used materials in the construction industry for its excellent mechanical properties and versatility [8–10]. However, concrete is not chemically stable at high temperatures [11], especially during accelerated, uncontrolled increases in temperature.

Concrete structures are fire resistant, which allows them to survive. However, the chemical instability of concrete requires concrete quality control and many repairs, and sometimes the chemical damage cannot be repaired/controlled, so the building must be demolished. This can occur in modern buildings, such as the eight-story building in Hengyang (China) that collapsed after enduring high temperatures in a fire, and buildings considered historical, where fire protection is insufficient, such as the fire in 2018 in the National Museum of Brazil in Rio de Janeiro, where the building was completely burned down [12].

The degradation of material properties under fire exposure conditions is one of the causes of failure of concrete structures [7] because cementitious composites are characterized by their low deformation capacity and weak tensile strength. The inclusion of fibers in the cementitious matrix allows improvement of this weakness [13]. The incorporation of fibers in concrete is a strategy to increase the safety requirements for buildings against fire events, where the durability of concrete structures are affected when they have been exposed to high temperatures and there are variations in the chemical and mechanical properties of the concrete [14–16]. Inclusion of fibers contributes to the reduction in cracks generated by concrete shrinkage [17], generating products with higher tensile strength, greater durability, ductility and toughness. Effectiveness of their incorporation depends on several factors, including fiber geometry, type, size, volume and dispersion [18,19].

In construction, steel and PP fibers are commonly employed, although recently there have been investigations on the inclusion of polyvinyl alcohol fibers [20,21]. The addition of steel fibers in concrete is the most employed method, which improves the mechanical behavior of concrete. Moreover, by performing a correct orientation of the steel fibers with the help of a magnetized bar, increases in almost all the mechanical properties of concrete are generated, such as compressive strength, flexural strength, shear strength, in addition to post-cracking properties and toughness [22].

Polyvinyl alcohol (PVA) fibers have high strength and ductility, in addition to excellent corrosion resistance without toxicity, improving the subsequent behavior of concrete after cracking and increasing its ductility and toughness. However, the incorporation of PVA fibers produces a significant decrease in the fluidity of concrete mixtures, generating higher porosity and affecting the matrix [20,21].

The incorporation of PP fibers generates a decrease in the workability of the mortar, due to the absorption of the cement paste caused by the surfaces of the fibers, generating the effect of fiber attachment [9]. However, when PP fiber-reinforced concrete is exposed to elevated temperatures, thermal stability is generated, preventing damage such as spalling [23], which is the product of the development of thermal stresses with the evaporation of free water, increasing the growth of interstitial pressure [2,24–26].

When the fibers reached a temperature of between 160–170 °C they melted and generated expansion channels, and these channels were created together with the additional porosity and allowed a decrease in the internal vapor pressure generated in the concrete, significantly reducing the probability of detachment. However, the additional porosity produced can produce decreases in the residual mechanical properties of the concrete [7,13,27,28].

The thermal incompatibility of concrete components generated by exposure to fire is the result of two mechanisms, one being the restricted thermal expansion mechanism and the vapor pressure build-up mechanism, producing thermal stresses between the expanding and contracting aggregate for the cement paste [13]. When concrete is exposed to high temperatures, significant changes occur in its internal structure, which leads to deterioration of the concrete, causing spalling at high temperatures and even failure of its components [29]. The mechanical properties of concrete depend on hydration products such as calcium silicate hydrate gel, calcium hydroxide and ettringite, which are formed during the hydration of cement and water. During a fire, concrete undergoes evaporation of the free water in its matrix [23]. When the temperature begins to increase, the disintegration of the hydrates begins, together with the water that is chemically bound, and the calcium hydroxide begins to decompose at 350 °C. At 500 °C the partial volatilization of the calcium silicate hydrate gel occurs, causing an increase in the porosity of the concrete and a decrease in its mechanical properties [13,30]. Research on the fire resistance of concrete has been carried out over the last decade, and many of these studies consider aspects such as aggregate types, fiber content, heating rate or maximum temperature level [31].

Many studies mention that the incorporation of PP fibers in the mix is one of the most effective solutions to reduce the risk of spalling of concrete or mortar that has been exposed to high temperature [7,23,32–38]. Investigations on the fire behaviors of concrete can be

the basis of a machine learning method, but experimental investigations are necessary to generate a suitable database for the models [39].

When a fire occurs, the PP fibers sublimate when they reach 170 °C, creating a network of micro channels in the concrete, which will serve as a channel for the release of vapor to the atmosphere, reducing mortar failure. The addition of PP fibers in the mix improves the spalling resistance of concrete or mortar at high temperatures [23,40], but it also has a negative effect on the remaining mechanical properties of the mortar, producing reductions in the remaining compressive strength, tensile strength and modulus of elasticity of the baked concrete [41,42].

Yermak et al. [43] carried out a study on the effect of the incorporation of steel and PP fibers in the preparation of concrete specimens when subjected to high temperatures, obtaining their mechanical properties. The resistance achieved was 70 MPa for the concrete used as a standard and showed spalling when exposed to high temperature. However, the concrete that combined PP fibers (0.75 kg/m³) and steel fibers (60 kg/m³) did not spall, having a residual compressive strength of 56 MPa at a temperature of 600 °C. It was concluded that the use of PP fibers increases the permeability and porosity of the concrete, resulting in a higher resistance to spalling.

The objective of this research is to analyze the mechanical properties of cement mortars reinforced with PP fibers when exposed to high temperatures and cooled in different regimes. Four dosages of cement mortars were elaborated, a reference sample without PP fibers and samples with the addition of PP fibers at 2, 3 and 4 kg/m³. The prepared specimens were exposed to temperatures of 20, 50, 100, 200, 300, 400 and 500 °C for one hour, and then cooled under different regimes to obtain their residual mechanical properties.

2. Materials and Methods

The cement used during the development of this research was CEM II/B-L 32.5 R, which complies with the requirements of the norm UNE EN 197-1 [44] and the recommendations of Real Decreto 256/2016 of the instruction for the reception of cements (RC-16) [45]. Table 1 details the characteristics of the cement used.

Table 1. Characteristics of CEM II/B-L 32.5.

Characteristics		
Clinker	65–79	%
Limestone	21–35	%
Minority components	0–5	%
Physical and mechanical characteristics		
Compressive strength	$\geq 32.5 \leq 52.5$	MPa
Onset of setting time	≥ 75	min.
Stability (expansion)	≤ 10	mm
Chemical properties		
Loss on calcination	No limitation	
Insoluble residue	No limitation	
Sulfate (SO ₃)	≤ 3.5	%
Chlorides (Cl ⁻)	≤ 0.1	%

The mortar was made with silica sand with a nominal maximum size of 4 mm. The density of the sand particles was 2320 kg/m³, and the fine aggregate had a fineness modulus of 3.9. The granulometry obtained was carried out according to that described in the norm UNE-EN 933-1 [46], and the test results are shown in Table 2.

The PP fibers used were monofilaments, complying with the standard UNE 14889-2 Clase 1-a: “Microfibra Mono filamentosa” [47], and the properties of the polypropylene fibers are listed in Table 3.

Table 2. Granulometry results.

Sieve Opening Size (mm)	4	2	1	0.5	0.25	0.125	0.063
Cumulative percentages passing (% in mass)	100	89	65	39	14	4	1

Table 3. Properties of polypropylene fibers.

Density (kg/L)	Quantity (Units/kg)	Length (mm)	Diameter (μm)	Tenacity (N/mm ²)	Melting Point ($^{\circ}\text{C}$)
0.91	102 million	12	31	280–310	163–170

Four types of mortar mixtures were dosed in proportions of 1:3:0.6 of cement, sand and natural water, respectively, and the cement mortars were reinforced with PP fiber in quantities of 2, 3 and 4 kg/m³. Table 4 shows the proportions used for the specimens of 40 mm \times 40 mm \times 160 mm specimens prepared. The mortars were prepared mechanically, following the steps of the standard specified in UNE EN 196-1 [48]. The cement was mixed with the fibers, for 30 s so that it could be homogenized, and then the water was incorporated and mixed at a slow speed for 30 s. The sand was added in the following 30 s while continuing to mix at a slow speed. The speed was changed to a faster speed for 30 s, and the mixing was stopped after 90 s. During the first 30 s all the mortar that had adhered to the side walls and bottom of the container was removed using a rubber spatula to maintain an homogeneous mixture, and finally the mixing was continued at a faster speed for 60 s. The use of nanotechnology in the preparation of the specimens would improve the bond between the fibers and the mortar matrix [49].

Table 4. Design of mortar mixes.

Mix	Fiber (kg)	Cement (kg)	Sand (kg)	Water (kg)	Density (kg/m ³)
M	0	450	1350	270	2140
M2	1.8	450	1350	270	2120
M3	2.7	450	1350	270	2080
M4	3.6	450	1350	270	2060

The mortars were placed in prismatic molds of 40 mm \times 40 mm \times 160 mm, which were vibrated for homogeneous compaction. The specimens were kept in the steel molds for 24 h at a temperature of 22 ± 2 $^{\circ}\text{C}$, and then demolded and placed in a humid curing chamber at a temperature of 20 ± 2 $^{\circ}\text{C}$ for 28 days (Figure 1). Three specimens were prepared for each of the dosages and each exposure temperature range, and this was multiplied by the two cooling regimes, resulting in the need for a total of 168 specimens to be prepared. Table 5 shows the variables used during the development of the investigation.

**Figure 1.** Elaborated mortar specimens.

Table 5. Variables used in the investigation.

Temperature (°C)	Polypropylene Fiber (Kg/m ³)	Cooling Regime
20, 50, 100, 200, 300, 400, 500	0, 2, 3, 4	air, water

After 28 days, the specimens were moved from the curing chamber and dried at room temperature for 96 h. They were then weighed and placed in an R-8 L electric muffle furnace (Figure 2), which had a power of 1800 W, an accuracy of ± 2 °C and reaches a maximum temperature capacity of 1100 °C. A heating rate of 15 °C/min was applied to the specimens until reaching temperatures of 50, 100, 200, 300, 400 and 500 °C, for one hour. Half of the specimens were kept under laboratory conditions (HR = 40%, T = 20 ± 2 °C) to be air cooled to room temperature. The rest were sharply cooled by submerging them in water until a temperature of 20 ± 3 °C was reached. After cooling, the mass values of the specimens were obtained, and they were tested for compression and flexure. The tests were carried out following the procedures described in norm UNE EN 196-1 [48]. The flexural strength tests were performed and then the compressive strength test was performed on the broken specimens.

**Figure 2.** R-8 L Electric Muffle Furnace.

3. Results and Discussion

The results obtained from the tests on the prepared specimens were used to check if there were variations in their mechanical properties when the specimens were exposed to high temperatures. In addition, whether there were differences in the mechanical properties according to the types of cooling the specimens experienced and finally, correlations between the flexural and compressive strength values without differentiating the cooling regimes were analyzed.

The densities of the processed mortars are shown in Table 4, where the increase in the amount of PP fibers produces a decrease in the mortar density. The results of the specimens reinforced with fibers and exposed to high temperatures were compared with the unreinforced specimens exposed to the same temperatures to obtain the mass loss, flexural strength and compressive strength. The masses of the specimens were obtained before and after being exposed to high temperatures, in addition to taking the masses after being cooled in air and water, and the differences between the masses before being exposed to temperature and after being cooled under their respective regimes were calculated for each temperature range, as presented in Figures 3 and 4.

The specimens reinforced with more fibers and exposed to high temperatures, showed mass decreases of a greater amount compared to the specimens without fibers. This is a result of two phenomena, i.e., the dehydration of $\text{Ca}(\text{OH})_2$ and the disintegration of the PP fibers.

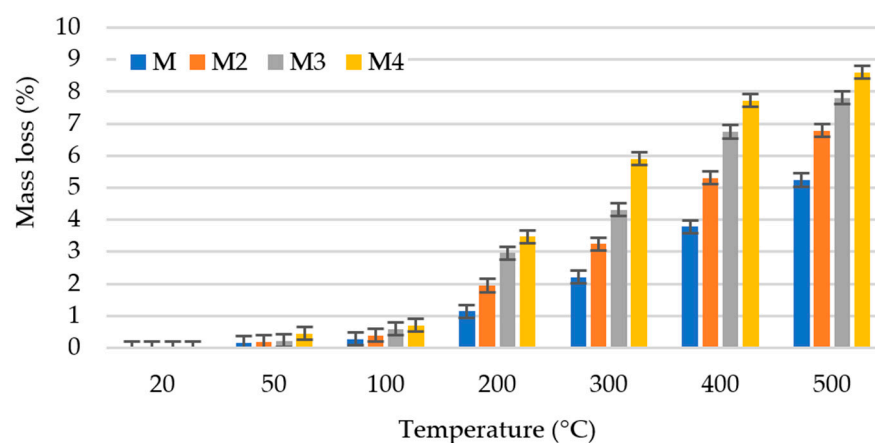


Figure 3. Percentages of the mass losses under the air regime.

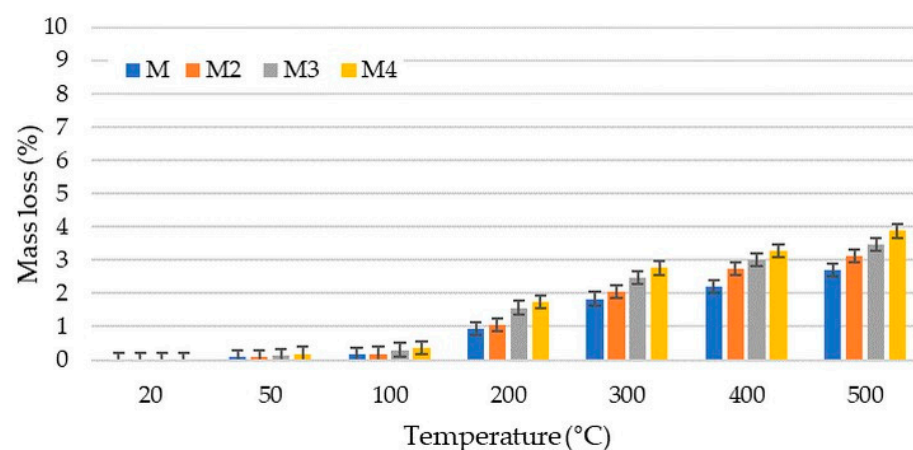


Figure 4. Percentages of the mass losses under the water regime.

Both figures show that the higher the amount of PP fibers in the mortar and the exposure to higher temperatures, the higher the percentage of mass loss is, both for the air and water regimes, having percentage mass losses between 5 to 9% and 2 to 4%, respectively, when reaching a temperature of 500 °C. The mass loss for the air cooling regime is greater than that obtained for the water regime, due to the dehydration of $\text{Ca}(\text{OH})_2$, producing CaO in the mortar, which causes a loss of mass in the specimens, and adding to this the disintegration of the PP fibers when they reach their melting temperature of 170 °C.

For the temperature range of 50 °C to 100 °C the specimens undergo evaporation of free water from the structure, so their mass changes are less than 1% for both cooling regimes. However, when the temperature exceeds 350 °C the process of $\text{Ca}(\text{OH})_2$ dehydration begins, due to the pressure generated by the evaporation of water, where explosive spalling can occur [23].

When the specimens are cooled under the water regime, they absorb water through the macropores left by the melting of the fibers, producing the rehydration of the CaO and generating an increase in the mass of the specimen. The mass loss presented corresponds to the product of the released water and the melted PP fibers. These results agree with the investigations [50–52], where they proved that there were mass losses in cement mortars when they were exposed to high temperatures, with a greater mass loss when the cooling regime was by air, in comparison to water.

The results of the flexural strength for each type of mix and each temperature range were obtained from testing series of three mortar specimens after being cooled under the different regimes, and the values shown in Table 6 belong to the arithmetic mean of the results obtained from each of the series, indicating that the higher the temperature, the more considerably the flexural strength decreases.

Table 6. Flexural strengths of the specimens cooled in air and water.

Mix	Cooling Regime	20 °C	50 °C	100 °C	200 °C	300 °C	400 °C	500 °C
M (MPa)	Air	7.00 ± 0.02	6.80 ± 0.02	5.94 ± 0.04	5.48 ± 0.06	5.02 ± 0.09	1.29 ± 0.03	0.11 ± 0.02
M2 (MPa)	Air	7.60 ± 0.03	7.51 ± 0.09	6.12 ± 0.15	5.70 ± 0.12	5.60 ± 0.16	1.39 ± 0.35	0.17 ± 0.09
M3 (MPa)	Air	7.65 ± 0.10	7.58 ± 0.25	5.56 ± 0.11	5.47 ± 0.06	5.20 ± 0.03	0.12 ± 0.01	0.05 ± 0.03
M4 (MPa)	Air	7.71 ± 0.05	7.55 ± 0.14	5.58 ± 0.19	5.24 ± 0.14	3.87 ± 0.37	0.08 ± 0.01	0.03 ± 0.01
M (MPa)	Water	6.95 ± 0.05	6.75 ± 0.05	5.90 ± 0.05	5.40 ± 0.04	5.12 ± 0.03	0.75 ± 0.03	0.05 ± 0.01
M2 (MPa)	Water	7.63 ± 0.22	7.45 ± 0.19	6.40 ± 0.33	5.73 ± 0.12	5.90 ± 0.39	0.88 ± 0.28	0.03 ± 0.02
M3 (MPa)	Water	7.66 ± 0.05	7.55 ± 0.19	5.60 ± 0.19	4.80 ± 0.22	4.50 ± 0.16	0.16 ± 0.07	0.02 ± 0.00
M4 (MPa)	Water	7.69 ± 0.10	7.52 ± 0.11	5.69 ± 0.39	3.86 ± 0.02	2.79 ± 0.15	0.12 ± 0.02	0.01 ± 0.00

With the results obtained for the flexural strengths, a statistical analysis was performed with Alpha = 0.05 based on the following hypotheses.

H₀: *There is no significant difference between the flexural strength values for the cooling regimes.*

H₁: *There is a significant difference between the flexural strength values for the cooling regimes.*

The analysis of the values shown in Table 7, determines with a probability ($0.28 > 0.05$) and Fisher's distribution ($1.15 < 4.07$) that there is no significant difference in the flexural strength values when the specimens are cooled in the air and water regimes, so statistically the type of cooling does not significantly influence their strength values.

Table 7. Statistical analysis on the flexural strengths of the specimens cooled in air and water.

Origin of Variations	F	Probability	Critical Value for F
Cooling regime	1.150655616	0.289536889	4.072653759
Temperature	229.6811767	1.85297×10^{-30}	2.323993797
Interaction	0.303979326	0.93135965	2.323993797

A probability of ($1.85 \times 10^{-30} < 0.05$) and Fisher's distribution ($229.7 > 2.32$), determines that there is a significant correlation between the values of flexural strengths and temperature ranges, i.e., the higher the temperature, the lower the strength values.

Finally, with a probability ($0.93 > 0.05$) and Fisher's distribution ($0.30 < 2.32$) the hypothesis H₀ is validated, there is no significant difference between the flexural strength values when the specimens are exposed to high temperatures and cooled under the air or water regimes, and thus, statistically the type of cooling does not directly influence their strength.

Figures 5 and 6 show the variations of the flexural strengths of the mortars in the different exposed temperature ranges.

The M specimens have lower flexural strength at room temperature, regardless of the cooling regimes, compared to M2, M3 and M4 specimens containing PP fibers. Under the air cooling regime when the analysis temperature was 50 °C, the variation of residual flexural strength was insignificant. This is the opposite when the analysis temperature is 100 °C, where there are reductions in the residual strength by 19% for M2, 27% in M3 and 28% in M4 along with the residual strength loss of 15% for specimen M that does not contain PP fiber reinforcement. As the temperature increases, the loss of residual strength is significant, and when reaching 200 °C the M2, M3 and M4 specimens present reductions in the residual strength of 25, 28 and 32%, respectively, being higher than the strength loss of the M specimen which is 22%. At 300 °C, the strength value of M is reduced by 28%, but its reduction is less compared to specimens M3 and M4, which are reduced by 32% and 50%, respectively, while M2 specimens have a 25% reduction in their strength, when the temperature is 400 °C. The reductions in the strength of specimens M, M2, M3 and M4 are 81.5, 81.7, 98.0 and 98.9%, respectively. When reaching a temperature of 500 °C, specimens M and M2 have reductions of 98.4 and 97.7% in their flexural strength, respectively, and

for specimens M3 and M4 their reductions reach almost 100%. The M2 specimens have lower reductions in strength compared to the M, M3 and M4 specimens, up to the heating temperature of 400 °C.

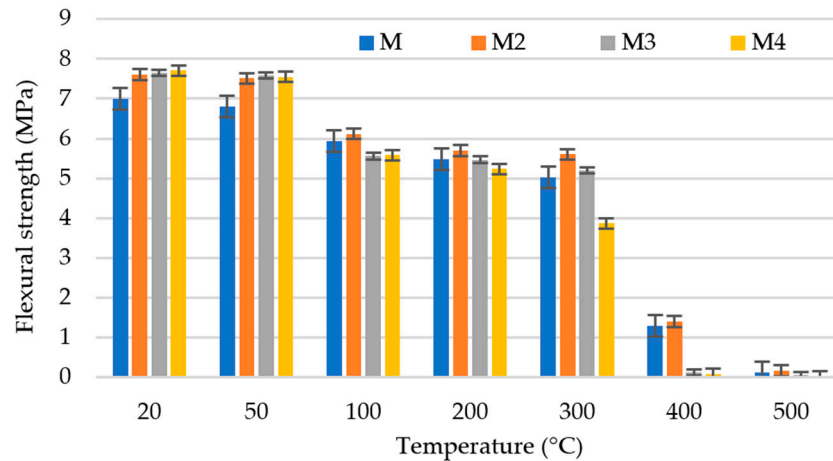


Figure 5. Flexural strengths subjected to high temperatures and the air cooling regime.

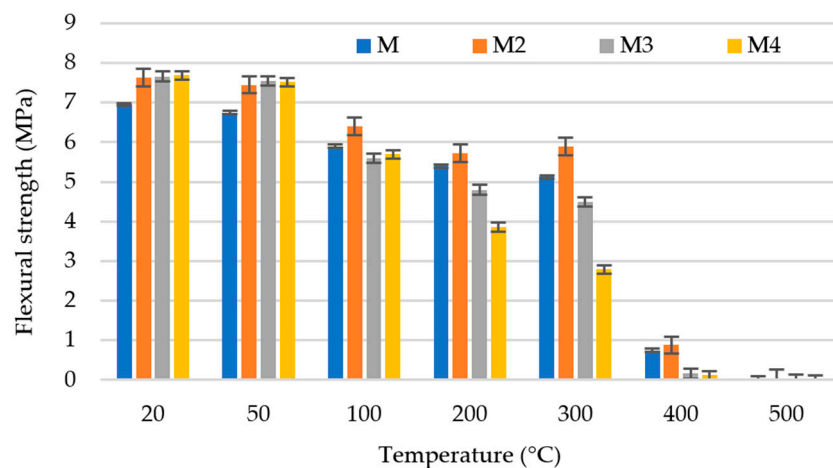


Figure 6. Flexural strengths subjected to high temperatures and the water cooling regime.

Under the water cooling regime, when the analysis temperature is 50 °C, the variation of residual flexural strength is insignificant. This becomes the opposite when the analysis temperature is 100 °C, where there are reductions of 16% for M2, 27% for M3 and 26% for M4 in the residual strength along with a percentage loss of the residual strength by 15% for specimen M that does not contain PP fiber reinforcement. As the temperature increases, the loss of residual strength is significant. When reaching 200°C, specimens M2, M3 and M4 sustain reductions of 25, 37 and 50% in residual strength, respectively, being higher than the percentage strength loss for specimen M which is 22%. At 300 °C, the strength value of M is reduced by 26%, but its reduction is less compared to specimens M3 and M4, which are reduced by 41% and 64%, respectively, while specimen M2 has a 23% reduction in its strength. When the temperature is 400 °C, the reductions in the strength for specimens M, M2, M3 and M4 are 89%, 88%, 98% and 98%, respectively, while reaching a temperature of 500 °C, specimens M, M2, M3 and M4 have reductions in their flexural strength by 100%. The M2 specimens have smaller reductions in strength compared to the M, M3 and M4 specimens, up to the heating temperature of 400 °C.

The specimens cooled under the air regime present a lower reduction in the flexural strength compared to the specimens cooled in water. The M2 specimens have higher flexural strength as temperatures increase up to 300 °C, regardless of the cooling regimes, and the

strength value is higher compared to the M, M3 and M4 specimens, which is consistent with the previous research [52,53], where it is indicated that specimens reinforced with a fiber content of 2 kg/m³ perform better in flexural strength.

In general, it is observed that the inclusion of PP fibers in quantities of 2, 3 and 4 kg/m³ to produce cement mortars, of type CEM II/B-L 32.5 does not favor the flexural strength when placed at temperatures higher than 500 °C.

The results of the compressive strength for each type of mix and each temperature range were obtained by testing a series of six mortar specimens after the flexural strength test. The values shown in Table 8 are the arithmetic means of the results obtained for individual series, where it is observed that the higher the exposed temperature, the lower the residual strength. For the specimens cooled in the water regime, they have the lowest residual compressive strength.

Table 8. Compressive strengths of the specimens cooled in air and water.

Mix	Cooling Regime	20 °C	50 °C	100 °C	200 °C	300 °C	400 °C	500 °C
M (MPa)	Air	31.76 ± 0.70	31.57 ± 0.81	30.90 ± 0.68	29.27 ± 0.22	28.43 ± 0.25	21.75 ± 0.39	18.62 ± 0.65
M2 (MPa)	Air	37.08 ± 0.27	36.22 ± 0.46	35.50 ± 0.50	34.54 ± 0.37	31.48 ± 0.48	24.67 ± 0.63	19.65 ± 0.58
M3 (MPa)	Air	37.46 ± 0.66	35.83 ± 0.36	28.49 ± 0.46	28.22 ± 0.45	27.84 ± 0.52	18.68 ± 0.47	16.90 ± 0.58
M4 (MPa)	Air	37.53 ± 0.43	35.49 ± 0.10	26.88 ± 0.72	24.68 ± 0.51	21.89 ± 0.99	17.12 ± 0.18	12.18 ± 0.11
M (MPa)	Water	32.09 ± 0.54	31.57 ± 0.58	29.07 ± 0.50	26.48 ± 0.32	25.64 ± 0.32	16.83 ± 0.32	13.31 ± 0.85
M2 (MPa)	Water	35.27 ± 0.21	34.06 ± 0.42	33.06 ± 0.47	32.78 ± 0.76	30.39 ± 0.96	16.47 ± 0.35	13.78 ± 0.60
M3 (MPa)	Water	36.47 ± 0.17	31.98 ± 0.82	26.66 ± 0.61	21.80 ± 0.84	21.08 ± 1.11	14.44 ± 0.17	12.18 ± 0.40
M4 (MPa)	Water	36.79 ± 0.39	31.41 ± 0.14	22.03 ± 0.76	20.84 ± 0.50	17.69 ± 0.53	13.65 ± 0.21	11.53 ± 0.14

With the results obtained for the flexural strengths, a statistical analysis is performed with Alpha = 0.05 based on the following hypotheses.

H₀: *There is no significant difference between the compressive strength values under the cooling regimes.*

H₁: *There is a significant difference between the compressive strength values under the cooling regimes.*

The analysis of the values shown in Table 9, determines with a probability ($0.0024 < 0.05$) and Fisher's distribution ($10.37 > 4.07$) that there is a significant difference in the compressive strength values when the specimens are cooled under the air and water regimes. Hence, statistically, the type of cooling does significantly influence its strength value.

Table 9. Statistical analysis on the compressive strengths of the specimens cooled in air and water.

Origin of Variations	F	Probability	Critical Value for F
Cooling regime	10.37114056	0.002472053	4.072653759
Temperature	26.55528701	8.2486×10^{-13}	2.323993797
Interaction	0.228943632	0.964946175	2.323993797

With a probability of ($8.25 \times 10^{-13} < 0.05$) and Fisher's distribution ($26.7 > 2.32$) the analysis determines that there is a significant difference between the values of compressive strengths for the temperature ranges. The higher the temperature, the lower the strength.

Finally, with a probability ($0.96 > 0.05$) and Fisher's distribution ($0.23 < 2.32$) the hypothesis H₃ is validated. There is no significant difference between the values of the compressive strength when the specimens are exposed to high temperatures and cooled in air or water mechanisms. Statistically, the type of cooling does not directly influence their strength.

Figures 7 and 8 show the variations of the compressive strength of the mortars in the different temperature ranges exposed.

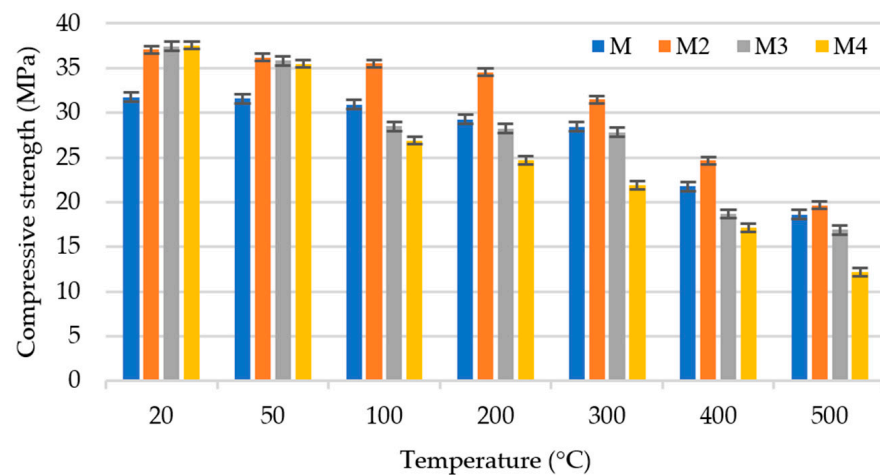


Figure 7. Compressive strengths of the specimens cooled under the air regime.

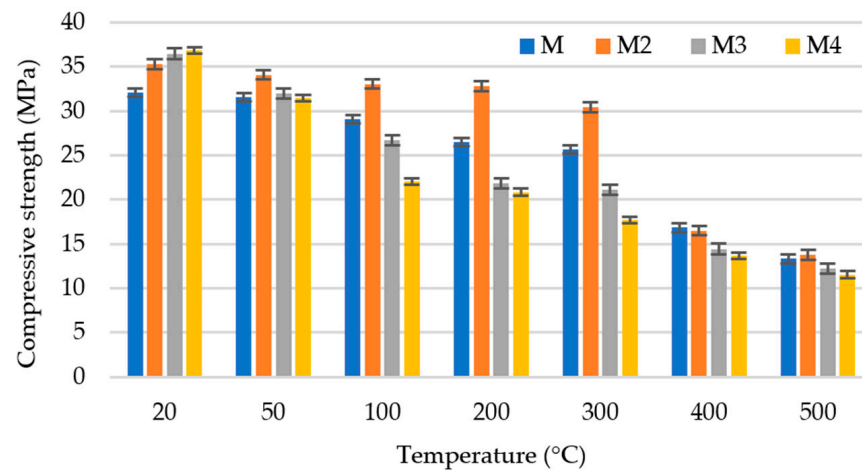


Figure 8. Compressive strengths of the specimens cooled under the water regime.

The M specimens have lower compressive strength at room temperature, regardless of the cooling regimes compared to M2, M3 and M4 specimens containing PP fibers. Under the air cooling regime, when the analysis temperature is 50 °C, small variations of residual compressive strength are observed, M2 specimens have a strength decrease of 2%, while M3 specimens have a decrease of 4%, and M4 specimens have a decrease of 5%. Compared to M specimens, the strength decreases by only 5%. When the analysis temperature is 100 °C, the residual strength sustains a 4% reduction for M2, 24% for M3 and 28% for M4 along with a percentage loss in the residual strength of 3% for the M specimen that does not contain PP fiber reinforcement. As the temperature increases, the loss of residual strength is significant. When 200 °C is reached, the M3 and M4 specimens present reductions of 25 and 34% in the residual strength, respectively, being higher than the percentage of loss of the M specimen, which is 8%. The opposite case occurs for the M2 specimens whose percentage of reduction is 7% of its residual strength compared to its initial value. However, its strength is still higher than the M, M3 and M4 specimens. At 300 °C, the compressive strength value of M is reduced by 10% from its initial value, but its reduction is minor compared to the strengths of specimens M3 and M4, which are reduced by 26 and 27%, respectively, from their initial values. Specimen M2 has a 15% reduction in its strength compared to its initial value, but its resistance remains higher than those of specimens M, M3 and M4. When the temperature is 400 °C, the reductions in the compressive strength for specimens M, M2, M3 and M4 were 32, 33%, 50% and 43%, respectively, in comparison with its values at a temperature of 20 °C. Despite the decrease in strength, specimen M2 has on average, a 22% compressive strength reduction in comparison with specimens M, M3 and M4 exposed

to 400 °C. When a temperature of 500 °C is reached, specimens M, M2, M3 and M4, have reductions of 41%, 47%, 55% and 68% in the compressive strength in relation to their values at the temperature of 20 °C. M2 specimens have a higher compressive strength relative to M, M3 and M4 specimens.

Under the water cooling regime, when the analysis temperature is 50 °C, small variations of the residual compressive strengths are observed, the compressive strength of M2 specimens decreases by 3%, while M3 specimens sustain a strength decrease of 12%, and M4 specimens sustain a compressive strength decrease of 15%, compared to the M specimens with a decrease of only 5%. When the analysis temperature is 100 °C, where residual strength reductions of 6% for M2, 27% in M3 and 40% in M4 occur, along with a residual strength loss percentage of 9% for the M specimen that does not contain PP fiber reinforcement. As the temperature increases, the loss of the residual strength is significant. When 200 °C is reached, specimens M3 and M4 sustain reductions of 40% and 43% in the residual strength, respectively, being higher than the percentage of loss of specimen R which is 17%, in contrast to specimen M2 whose percentage reduction is 7% in residual strength compared to its initial value, but its strength is still higher than those of specimens M, M3 and M4. At 300 °C, the compressive strength value of M is reduced by 20% with respect to its initial value, but its reduction is smaller compared to specimens M3 and M4, whose compressive strengths are reduced by 42% and 52%, respectively, from their initial values. Specimen M2 has a reduction of 14% in its strength compared to its initial value, but its strength remains higher than those of the M, M3 and M4 specimens. When the temperature is 400 °C, the reductions in the compressive strengths for the M, M2, M3 and M4 specimens are 48%, 53%, 60% and 63%, respectively, compared to their values at a temperature of 20 °C. Despite the decrease in the strength, specimen M2 has on average an 11% higher compressive strength compared to specimens M, M3 and M4 exposed to 400 °C. When reaching the heating temperature of 500 °C, the M, M2, M3 and M4 specimens have reductions of 59%, 61%, 67% and 69% in the compressive strength in relation to their values at a temperature of 20 °C. The M2 specimens have a higher compressive strength in relation to the M, M3 and M4 specimens.

The specimens cooled under the air regime have a higher compressive strength compared to the specimens cooled in water. In general, it is observed that the inclusion of PP fibers at a level of 2 kg/m³ for the preparation of cement mortars, type CEM II/B-L 32.5 favors the compressive strength, regardless of the cooling regimes, preventing spalling caused by high temperatures [54]. This is in agreement with the previous research [12,45,53,55], where it was indicated that specimens reinforced with a fiber content of 2 kg/m³ have a better performance in compressive strength.

The results showing the mechanical properties of the flexural and compressive strengths agree with previous research [8,33,56], where it is mentioned that the amount of 2 kg/m³ of PP fibers was the optimum content to achieve an improvement in fire resistance.

The correlation analysis between the values of compressive strength (R_c) and residual flexural strength (R_f) shown in Figure 9, indicates a linear regression of the expression $R_f = 0.35R_c - 4.40$ (MPa), with a coefficient of determination of $R^2 = 0.82$, which suggests that there is a good relationship between the variables studied, regardless of the temperature range exposed and the types of cooling used.

The effect of elevated temperatures on cement mortars is due to the alteration of its compounds such as ettringite, calcium silicate hydrate, Ca(OH)_2 and other components, at high temperatures, undergo dehydration, decarbonization and decomposition, resulting in new components such as calcium aluminate, calcium oxide and others [57–59], which are chemically altered in the post-fire stage, generating changes in the microstructure and mechanical properties, generating positive or negative effects on the post-fire cement mortars [60,61]. The losses of flexural and compressive strengths are due to the rehydration of CaO, transforming it into Ca(OH)_2 , and producing a reduction in the strength.

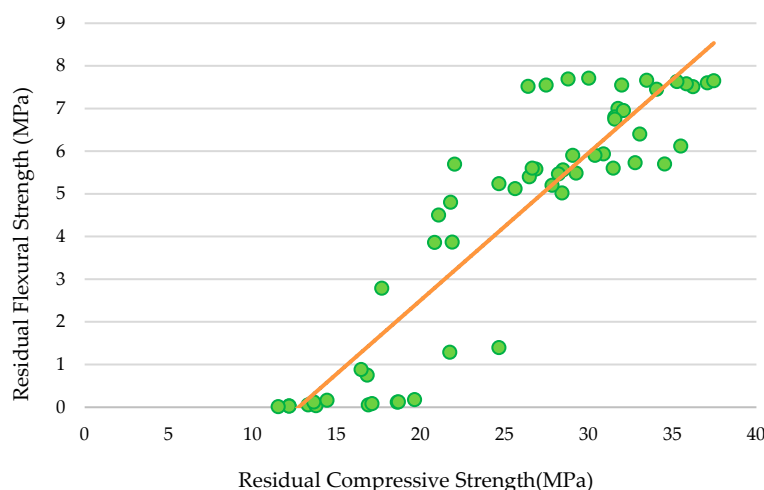


Figure 9. Correlation between the compressive and flexural strengths.

4. Conclusions

The mechanical properties of PP fiber-reinforced mortars when exposed to high temperatures were investigated. In addition to analyzing the influence of the types of cooling on the mechanical properties of the mortars, we finally reviewed the existence of a correlation between the residual flexural and compressive strengths regardless of the cooling regime.

- The exposure of the specimens to fire generates a loss of mass in the mortars. When the specimens reach 500 °C the loss of mass under the air cooling regime is approximately 7%, compared to the specimens cooled under the water regime where the mass reduction is approximately 3%. This is due to the dehydration of $\text{Ca}(\text{OH})_2$, producing CaO in the mortars cooled under the air regime, while under the water cooling regime, CaO rehydration occurs and generates an increase in mass in the specimens.
- The addition of 2 kg/m³ PP fibers increases the mechanical properties of the mortars compared to the other dosages. At a heating temperature of 300 °C the M2 specimens have a residual flexural strength of approximately 75% of the original strength, which is 15% higher than that observed in the simple mortar. The same happens with the residual compressive strength which was approximately 85% of the original strength, being 17% higher than that observed in the simple mortar.
- With the probability analysis and Fisher's distribution it can be concluded that there is no significant difference between the values of the residual flexural and compressive strengths when the specimens are exposed to high temperatures and cooled under the air or water regimes. Statistically, the type of cooling does not directly influence their strength.
- There is a correlation between the residual flexural and compressive strengths regardless of the cooling regime, with a coefficient of determination as $R^2 = 0.82$, which considers the relationship between the variables acceptable.
- It is recommended that research on the affectation of the flexural and compressive energy absorption capacities of PP fiber-reinforced mortars exposed to high temperatures and cooled under different regimes be carried out.

Author Contributions: Conceptualization, A.C. and Y.A.; methodology, M.I.P. and A.C.; software, Y.A.; validation, A.C., Y.A. and M.I.P.; formal analysis, A.C.; investigation, M.I.P.; resources, A.C.; data curation, Y.A.; writing—original draft preparation, Y.A.; writing—review and editing, M.I.P.; visualization, Y.A.; supervision, A.C.; project administration, M.I.P. All authors have read and agreed to the published version of the manuscript.

Funding: This research received no external funding.

Data Availability Statement: The data presented in this study are available on request from the corresponding author. The data are not publicly available due to privacy.

Conflicts of Interest: The authors declare no conflict of interest.

References

1. Ibrahim, H.A.; Mahdi, M.B.; Abbas, B.J. Mechanical properties of lightweight aggregate moderate strength concrete reinforcement with hybrid fibers. *Mater. Sci. Eng.* **2021**, *584*, 012048. [[CrossRef](#)]
2. Liu, L.; Yang, G.; He, J.; Liu, H.; Gong, J.; Yang, H.; Yang, W.; Joyklad, P. Impact of fibre factor and temperature on the mechanical properties of blended fibre-reinforced cementitious composite. *Case Stud. Constr. Mater.* **2022**, *16*, e00773. [[CrossRef](#)]
3. Wang, Z.; Han, S.; Sun, P.; Liu, W.; Wang, Q. Mechanical properties of polyvinyl alcohol-basalt hybrid fiber engineered cementitious composites with impact of elevated temperatures. *J. Cent. South Univ.* **2021**, *28*, 1459–1475. [[CrossRef](#)]
4. Chindaprasirt, P.; Boonbamrung, T.; Poolsong, A.; Kroehong, W. Effect of elevated temperature on polypropylene fiber reinforced alkali-activated high calcium fly ash paste. *Case Stud. Constr. Mater.* **2021**, *15*, e00554. [[CrossRef](#)]
5. Al-Rousan, R.Z. Impact of elevated temperature and anchored grooves on the shear behavior of reinforced concrete beams strengthened with CFRP composites. *Case Stud. Constr. Mater.* **2021**, *14*, e00487. [[CrossRef](#)]
6. Deng, Z.; Liu, X.; Yang, X.; Liang, N.; Yan, R.; Chen, P.; Miao, Q.; Xu, Y. A study of tensile and compressive properties of hybrid basalt-polypropylene fiber-reinforced concrete under uniaxial loads. *Struct. Concr.* **2021**, *22*, 396–409. [[CrossRef](#)]
7. Song, C.; Zhang, G.; Lu, Z.; Li, X.; Zhao, X. Fire resistance tests on polypropylene-fiber-reinforced prestressed concrete box bridge girders. *Eng. Struct.* **2023**, *282*, 115800. [[CrossRef](#)]
8. Nuaklong, P.; Boonchoo, N.; Jongvivatsakul, P.; Charinpanitkul, T.; Sukontasukkul, P. Hybrid effect of carbon nanotubes and polypropylene fibers on mechanical properties and fire resistance of cement mortar. *Constr. Build. Mater.* **2021**, *275*, 122189. [[CrossRef](#)]
9. Chen, G.; Gao, D.; Zhu, H.; Yuan, J.S.; Xiao, X.; Wang, W. Effects of novel multiple hooked-end steel fibres on flexural tensile behaviour of notched concrete beams with various strength grades. *Structures* **2021**, *33*, 3644–3654. [[CrossRef](#)]
10. Gao, D.; Gu, Z.; Wei, C.; Wu, C.; Pang, Y. Effects of fiber clustering on fatigue behavior of steel fiber reinforced concrete beams. *Constr. Build. Mater.* **2021**, *301*, 124070. [[CrossRef](#)]
11. Ogrodnik, P.; Szulej, J. The impact of aeration of concrete based on ceramic aggregate, exposed to high temperatures, on its strength parameters. *Constr. Build. Mater.* **2017**, *157*, 909–916. [[CrossRef](#)]
12. Müller, P.; Novák, J.; Holan, J. Destructive and non-destructive experimental investigation of polypropylene fibre reinforced concrete subjected to high temperature. *J. Build. Eng.* **2019**, *26*, 100906. [[CrossRef](#)]
13. Çavdar, A. A study on the effects of high temperature on mechanical properties of fiber reinforced cementitious composites. *Compos. B Eng.* **2012**, *43*, 2452–2463. [[CrossRef](#)]
14. Chiadighikaobi, P.C. Effects of basalt fiber in lightweight expanded clay concrete on compressive strength and flexural strength of lightweight basalt fiber reinforced concrete. *IOP Conf. Ser. Mater. Sci. Eng.* **2019**, *640*, 012055. [[CrossRef](#)]
15. Haddad, R.H.; Shannis, L.G. Post-fire behavior of bond between high strength pozzolanic concrete and reinforcing steel. *Constr. Build. Mater.* **2004**, *18*, 425–435. [[CrossRef](#)]
16. Balgourinejad, N.; Haghighifar, M.; Madandoust, R.; Charkhtab, S. Experimental study on mechanical properties, microstructural of lightweight concrete incorporating polypropylene fibers and metakaolin at high temperatures. *J. Mater. Res. Technol.* **2022**, *18*, 5238–5256. [[CrossRef](#)]
17. Adesina, A. Performance of cementitious composites reinforced with chopped basalt fibres—An overview. *Constr. Build. Mater.* **2021**, *266*, 120970. [[CrossRef](#)]
18. Mehta, P.K.; Monteiro, P.J.M. *Concrete—Microstructure, Properties, and Materials*, 4th ed.; McGraw Hill Education: New York, NY, USA, 2014.
19. Kuder, K.G.; Shah, S.P. Processing of high-performance fiber-reinforced cement-based composites. *Constr. Build. Mater.* **2010**, *24*, 181–186. [[CrossRef](#)]
20. Zhang, X.; Wu, X.; Wang, Y. Corrosion-effected bond behavior between PVA-fiber-reinforced concrete and steel rebar under chloride environment. *Materials* **2023**, *16*, 2666. [[CrossRef](#)]
21. Zhang, X.; Lu, Q.; Wang, Y. Experimental study on bond behavior between steel rebar and PVA fiber-reinforced concrete. *Coatings* **2023**, *13*, 740. [[CrossRef](#)]
22. Zhang, X.; He, F.; Chen, J.; Yang, C.; Xu, F. Orientation of steel fibers in concrete attracted by magnetized rebar and its effects on bond behavior. *Cem. Concr. Compos.* **2023**, *138*, 104977. [[CrossRef](#)]
23. Durgun, M.Y.; Özen, S.; Karakuzu, K.; Kobya, V.; Bayqra, S.H.; Mardani-Aghabaglou, A. Effect of high temperature on polypropylene fiber-reinforced mortars containing colemanite wastes. *Constr. Build. Mater.* **2022**, *316*, 125827. [[CrossRef](#)]
24. Liu, J.; Tan, K.H.; Yao, Y. A new perspective on nature of fire-induced spalling in concrete. *Constr. Build. Mater.* **2018**, *184*, 581–590. [[CrossRef](#)]
25. Zhang, H.Y.; Qiu, G.H.; Kodur, V.; Yuan, Z.S. Spalling behavior of metakaolin-fly ash based geopolymer concrete under elevated temperature exposure. *Cem. Concr. Compos.* **2020**, *106*, 103483. [[CrossRef](#)]
26. Holan, J.; Novák, J.; Müller, P.; Štefan, R. Experimental investigation of the compressive strength of normal-strength air-entrained concrete at high temperatures. *Constr. Build. Mater.* **2020**, *248*, 118662. [[CrossRef](#)]
27. Han, C.; Hwang, Y.; Yang, S.; Gowripalan, N. Performance of spalling resistance of high performance concrete with polypropylene fiber contents and lateral confinement. *Cem. Concr. Res.* **2005**, *35*, 1747–1753. [[CrossRef](#)]

28. Poon, C.S.; Shui, Z.H.; Lam, L. Compressive behavior of fiber reinforced high-performance concrete subjected to elevated temperatures. *Cem. Concr. Res.* **2004**, *34*, 2215–2222. [[CrossRef](#)]
29. Li, D.; Niu, D.; Fu, Q.; Luo, D. Fractal characteristics of pore structure of hybrid Basalt–Polypropylene fibre-reinforced concrete. *Cem. Concr. Comp.* **2020**, *109*, 103555. [[CrossRef](#)]
30. Bošnjak, J.; Ožbolt, J.; Hahn, R. Permeability measurement on high strength concrete without and with polypropylene fibers at elevated temperatures using a new test setup. *Cem. Concr. Res.* **2013**, *53*, 104–111. [[CrossRef](#)]
31. Poon, C.; Azhar, S.; Anson, M.; Wong, Y. Comparison of the strength and durability performance of normal- and high-strength pozzolanic concretes at elevated temperatures. *Cem. Concr. Res.* **2001**, *31*, 1291–1300. [[CrossRef](#)]
32. He, F.; Biolzi, L.; Carvelli, V. Effects of elevated temperature and water re-curing on the compression behavior of hybrid fiber reinforced concrete. *J. Build. Eng.* **2023**, *67*, 106034. [[CrossRef](#)]
33. Aydın, S.; Yazıcı, H.; Baradan, B. High temperature resistance of normal strength and autoclaved high strength mortars incorporated polypropylene and steel fibers. *Constr. Build. Mater.* **2008**, *22*, 504–512. [[CrossRef](#)]
34. Peng, G.; Yang, W.; Zhao, J.; Liu, Y.; Bian, S.; Zhao, L. Explosive spalling and residual mechanical properties of fiber-toughened high-performance concrete subjected to high temperatures. *Cem. Concr. Res.* **2006**, *36*, 723–727. [[CrossRef](#)]
35. Xiao, J.; König, G. Study on concrete at high temperature in China—An overview. *Fire Saf. J.* **2004**, *39*, 89–103. [[CrossRef](#)]
36. Khaliq, W.; Kodur, V. Thermal and mechanical properties of fiber reinforced high performance self-consolidating concrete at elevated temperatures. *Cem. Concr. Res.* **2011**, *41*, 1112–1122. [[CrossRef](#)]
37. Jang, H.; So, H.; So, S. The properties of reactive powder concrete using PP fiber and pozzolanic materials at elevated temperature. *J. Build. Eng.* **2016**, *8*, 225–230. [[CrossRef](#)]
38. Lura, P.; Terrasi, G.P. Reduction of fire spalling in high-performance concrete by means of superabsorbent polymers and polypropylene fibers: Small scale fire tests of carbon fiber reinforced plastic-prestressed self-compacting concrete. *Cem. Concr. Comp.* **2014**, *49*, 36–42. [[CrossRef](#)]
39. Kioumars, M.; Dabiri, H.; Kandiri, A.; Farhangi, V. Compressive strength of concrete containing furnace blast slag; optimized machine learning-based models. *Clean. Eng. Technol.* **2023**, *13*, 100604. [[CrossRef](#)]
40. Abaeian, R.; Behbahani, H.P.; Moslem, S.J. Effects of high temperatures on mechanical behavior of high strength concrete reinforced with high performance synthetic macro polypropylene (HPP) fibres. *Constr. Build. Mater.* **2018**, *165*, 631–638. [[CrossRef](#)]
41. Rodrigues, J.P.C.; Laím, L.; Correia, A.M. Behaviour of fiber reinforced concrete columns in fire. *Compos. Struct.* **2010**, *92*, 1263–1268. [[CrossRef](#)]
42. Sideris, K.K.; Manita, P.; Chaniotakis, E. Performance of thermally damaged fibre reinforced concretes. *Constr. Build. Mater.* **2009**, *23*, 1232–1239. [[CrossRef](#)]
43. Yermak, N.; Pliya, P.; Beaucour, A.; Simon, A.; Noumowé, A. Influence of steel and/or polypropylene fibres on the behaviour of concrete at high temperature: Spalling, transfer and mechanical properties. *Constr. Build. Mater.* **2017**, *132*, 240–250. [[CrossRef](#)]
44. EN 197-1:2011; Cement—Part 1: Composition, Specifications and Conformity Criteria for Common Cements. AENOR: Madrid, Spain, 2011.
45. Ministerio de la Presidencia. *Real Decreto 256/2016. Instrucción Para La Recepción de Cementos (RC-16)*; Agencia Estatal Boletín Oficial del Estado: Madrid, Spain, 2016.
46. EN 933-1:2012; Tests for Geometrical Properties of Aggregates—Part 1: Determination of Particle Size Distribution—Sieving Method. AENOR: Madrid, Spain, 2012.
47. EN 14889-2:2008; Fibres for Concrete—Part 2: Polymer Fibres—Definitions, Specifications and Conformity. AENOR: Madrid, Spain, 2008.
48. EN 196-1:2018; Methods of Testing Cement—Part 1: Determination of Strength. AENOR: Madrid, Spain, 2018.
49. Karakouzian, M.; Farhangi, V.; Farani, M.R.; Joshaghani, A.; Zadehmohamad, M.; Ahmadzadeh, M. Mechanical characteristics of cement paste in the presence of carbon nanotubes and silica oxide nanoparticles: An experimental study. *Materials* **2021**, *14*, 1347. [[CrossRef](#)] [[PubMed](#)]
50. Xiao, J.; Falkner, H. On residual strength of high-performance concrete with and without polypropylene fibres at elevated temperatures. *Fire Saf. J.* **2006**, *41*, 115–121. [[CrossRef](#)]
51. Zheng, W.; Luo, B.; Wang, Y. Microstructure and mechanical properties of RPC containing PP fibres at elevated temperatures. *Mag. Concr. Res.* **2014**, *66*, 397–408. [[CrossRef](#)]
52. Karahan, O.; Durak, U.; İlkentapar, S.; Atabey, İ.İ.; Atiş, C.D. Resistance of polypropylene fibered mortar to elevated temperature under different cooling regimes. *Rev. Constr.* **2019**, *18*, 386–397. [[CrossRef](#)]
53. Behnood, A.; Ghandehari, M. Comparison of compressive and splitting tensile strength of high-strength concrete with and without polypropylene fibers heated to high temperatures. *Fire Saf. J.* **2009**, *44*, 1015–1022. [[CrossRef](#)]
54. Amancio, F.A.; de Carvalho Rafael, M.F.; de Oliveira Dias, A.R.; Bezerra Cabral, A.E. Behavior of concrete reinforced with polypropylene fiber exposed to high temperatures. *Procedia Struct. Integr.* **2018**, *11*, 91–98. [[CrossRef](#)]
55. Ezziane, M.; Kadri, T.; Molez, L.; Jauberthie, R.; Belhacen, A. High temperature behaviour of polypropylene fibres reinforced mortars. *Fire Saf. J.* **2015**, *71*, 324–331. [[CrossRef](#)]
56. Pothisiri, T.; Soklin, C. Effects of mixing sequence of polypropylene fibers on spalling resistance of normal strength concrete. *Eng. J.* **2014**, *18*, 55–64. [[CrossRef](#)]

57. He, F.; Biolzi, L.; Carvelli, V. Effects of elevated temperature and water re-curing on fracture process of hybrid fiber reinforced concretes. *Eng. Fract. Mech.* **2022**, *276*, 108885. [[CrossRef](#)]
58. Awal, A.S.M.A.; Shehu, I.A.; Ismail, M. Effect of cooling regime on the residual performance of high-volume palm oil fuel ash concrete exposed to high temperatures. *Constr. Build. Mater.* **2015**, *98*, 875–883. [[CrossRef](#)]
59. Saridemir, M.; Severcan, M.H.; Ciflikli, M.; Celikten, S.; Ozcan, F.; Atis, C.D. The influence of elevated temperature on strength and microstructure of high strength concrete containing ground pumice and metakaolin. *Constr. Build. Mater.* **2016**, *124*, 244–257. [[CrossRef](#)]
60. Shui, Z.; Xuan, D.; Wan, H.; Cao, B. Rehydration reactivity of recycled mortar from concrete waste experienced to thermal treatment. *Constr. Build. Mater.* **2008**, *22*, 1723–1729. [[CrossRef](#)]
61. Poon, C.; Azhar, S.; Anson, M.; Wong, Y. Strength and durability recovery of fire-damaged concrete after post-fire-curing. *Cem. Concr. Res.* **2001**, *31*, 1307–1318. [[CrossRef](#)]

Disclaimer/Publisher’s Note: The statements, opinions and data contained in all publications are solely those of the individual author(s) and contributor(s) and not of MDPI and/or the editor(s). MDPI and/or the editor(s) disclaim responsibility for any injury to people or property resulting from any ideas, methods, instructions or products referred to in the content.